Inorg. Chem. **2007**, *46*, 1027−1032

Study of the Replacement of Weak Ligands on Square-Planar Organometallic Nickel(II) Complexes. Organo-Nickel Aquacomplexes

Juan A. Casares, Pablo Espinet,* Jesús M. Martínez-Ilarduya, Jesús J. Mucientes, and Gorka Salas

Química Inorgánica, Facultad de Ciencias, Universidad de Valladolid, E-47011 Valladolid, Spain

Received October 10, 2006

When *trans*-[$NiRf_2L_2$] (Rf = 3,5-$C_6Cl_2F_3$; L = group 15 soft monodentate weak ligand such as $SbPh_3$ or $AsPh_3$) is dissolved in wet $(CD_3)_2CO$, isomerization (to give *cis*-[$NiRf_2L_2$]) and subsequent substitutions of L by $(CD_3)_2CO$ or by water occur, and several complexes containing acetone and aqua ligands are formed. The isomerization takes place in a few seconds at room temperature. The substitution reactions on the cis isomer formed are faster. The kinetics of the equilibria between all of the participating species have been studied by ^{19}F exchange spectroscopy experiments at 217 K, and the exchange rates and rate constants have been calculated. These data reflect the weakness of acetone compared to water and $AsPh_3$. The data obtained are the first available for square-planar nickel(II) aquacomplexes. The bulkier $AsCyPh_2$ ligand slows down the exchange processes while the displacement of $AsMePh_2$ is clearly disfavored. Activation entropy studies support an associative ligand substitution. All of these data fit well with the previously reported relative activity of these complexes as catalysts in norbornene polymerization.

Introduction

Aquacomplexes of group 10 elements are of importance because of their involvement as catalysts or as intermediates in a number of processes.[1] The increasing interest in metal-mediated synthesis in water adds relevance to these aquacomplexes.[2]

In the course of our work on polyfluorophenyl complexes of group 10 elements, we have synthesized several complexes containing weakly coordinating neutral ligands that can be replaced by water.[3] In fact, the $(CD_3)_2CO$ solutions of *cis*-[$MRf_2(THF)_2$] (M = Pd, Pt; Rf = 3,5-$C_6Cl_2F_3$; THF = tetrahydrofuran) consist of a mixture of *cis*-[$MRf_2\{OC(CD_3)_2\}_2$], *cis*-[$MRf_2\{OC(CD_3)_2\}(OH_2)$], and *cis*-[$MRf_2(OH_2)_2$] in ratios that depend on the H_2O content in the deuterated solvent. The exchange between these complexes is fast in the NMR time scale at room temperature for M = Pd and too slow to be detected for M = Pt. A behavior quite similar to that of the palladium complex is observed for *trans*-[$NiRf_2(SbPh_3)_2$] (**1a**), an excellent catalyst for vinylic polymerization of norbornene.[4] Square-planar coordination in Ni(II) is favored in organometallic complexes. On the other hand, organo-nickel aquacomplexes are extremely uncommon due to the inherent high reactivity of Ni−C bonds toward hydrolysis.[5] For this reason, while water and solvent exchange processes are well-studied for octahedral complexes $[Ni(solv)_6]^{2+}$ (solv = H_2O, DMF, CH_3CN),[6,7] no data have been reported for nickel(II) square-planar organometallic compounds. Moreover, no crystal structures have been reported for organo-nickel aquacomplexes although the structures of some hydroxo-derivatives have been determined.[8]

In contrast to the high reactivity of conventional Ni−C bonds, the Ni−Rf bonds are exceptionally inert toward hydrolysis, which makes them perfectly suited substrates for

* To whom correspondence should be addressed. E-mail: espinet@qi.uva.es.

(1) Vicente, J.; Arcas, A. *Coord. Chem. Rev.* **2005**, *249*, 1135−1154.
(2) For interest in water as the solvent for reactions see: (a) *Aqueous-Phase Organometallic Catalysis: Concepts and Applications*, 2nd ed.; Cornils, B., Herrmann, W. A., Eds.; Wiley−VCH: Weinheim, Germany, 2004. (b) Shaughnessy, K. H.; DeVasher, R. B. *Curr. Org. Chem.* **2005**, *9*, 585−604. (c) Leadbeater, N. E. *Chem. Commun.* **2005**, 2881−2902.
(3) Espinet, P.; Martínez-Ilarduya, J. M.; Pérez-Briso, C.; Casado, A. L.; Alonso, M. A. *J. Organomet. Chem.* **1998**, *551*, 9−20.
(4) Casares, J. A.; Espinet, P.; Martín-Alvarez, J. M.; Martínez-Ilarduya, J. M.; Salas, G. *Eur. J. Inorg. Chem.* **2005**, 3825−3831.
(5) Koelle, U. *Coord. Chem. Rev.* **1994**, *135/136*, 623−650.
(6) (a) Ducommun, Y.; Newmann, K. E.; Merbach, A. E. *Inorg. Chem.* **1980**, *19*, 3696−3703. (b) Ducommun, Y.; Earl, W. L.; Merbach, A. E. *Inorg. Chem.* **1979**, *18*, 2754−2758.
(7) (a) Wilkins, R. G. *Kinetics and Mechanism of Reactions of Transition Metal Complexes*, 2nd ed.; VCH: Weinheim, Germany, 1991. (b) Dunand, F. A.; Helm, L.; Merbach, A. E. *Adv. Inorg. Chem.* **2003**, *54*, 1−69. (c) Helm, L.; Merbach, A. E. *Chem. Rev.* **2005**, *105*, 1923−1959.

10.1021/ic061933k CCC: $37.00
Published on Web 01/10/2007

Scheme 1

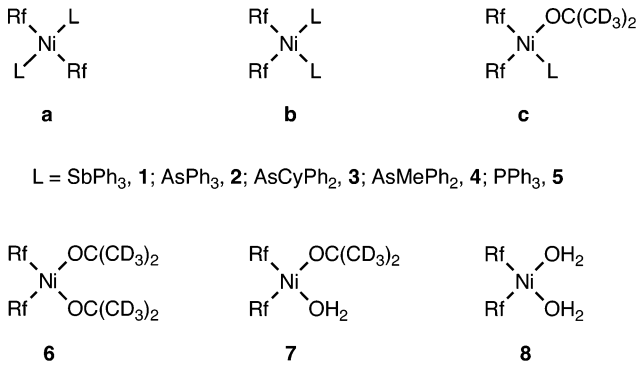

the study of other reactions, particularly substitution reactions involving water in square-planar Ni complexes. This prompted us to study the equilibria and exchange rates between the different species that coexist in solution when **1a** or other related *trans*-[$NiRf_2L_2$] complexes (L = $AsPh_3$, **2a**; $AsCyPh_2$, **3a**; $AsMePh_2$, **4a**; PPh_3, **5a**) are dissolved in wet $(CD_3)_2CO$. These are shown in Scheme 1.

^{19}F EXSY (exchange spectroscopy) experiments were used for the quantitative evaluation of the kinetics of these equilibria, since two-dimensional (2D) EXSY is appropriate to study multisite exchanges and dynamic processes that are slow in the chemical shift time scale.[9−11] Examples of the application of EXSY in organometallic and transition metal chemistry, often including their use to obtain quantitative kinetic data, are available in the literature.[12]

Results and Discussion

The complexes *trans*-[$NiRf_2L_2$] (**1a**−**5a**) are stable in the solid state, but they slowly decompose in a solution of $CDCl_3$ or $(CD_3)_2CO$ at 298 K to give Rf−Rf, RfH, and small amounts of other non-characterized products. The synthesis and behavior as catalysts of these complexes have been reported, as well as the X-ray structures of **1a**, **2a**, and **5a** that show a square-planar trans geometry for all of them.[4]

Since the room-temperature spectra of complexes **1a**−**5a** in the $CDCl_3$ solution were the same as the spectra recorded at 213 K from solid samples dissolved at low temperature (only the trans isomer is present in the solid state), it can be concluded that these solutions contain the trans isomer only, at least in a detectable concentration. Related complexes with aryl phosphines also show preference for trans stereochemistry, as found for [$Ni(C_6F_5)_2(PMePh_2)_2$] and [$Ni(4\text{-}C_6BrF_4)_2(PMePh_2)_2$] in solution ($CDCl_3$ or CD_2Cl_2) and in the solid state.[13−15] In contrast, only the cis isomers are obtained for complexes involving less sterically demanding ligands, such as [PPh_3Me][$Ni(C_6F_5)_2Br(CO)$], [$Ni(C_6F_5)_2(CO)_2$], and [$Ni(C_6F_5)_2(THF)_2$].[16]

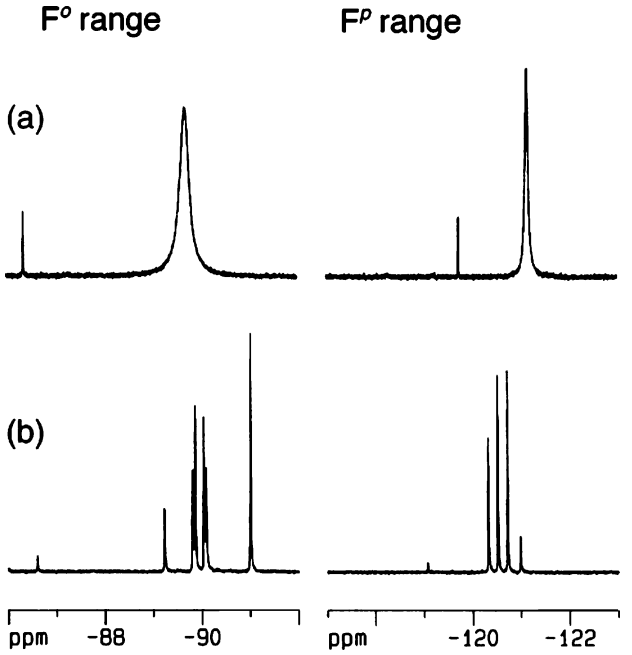

Figure 1. ^{19}F NMR spectra of a solution of *trans*-[$NiRf_2(SbPh_3)_2$] (**1a**) in wet $(CD_3)_2CO$ at 293 K (a) and 217 K (b).

Behavior in Acetone-d_6 Solution. The ^{19}F NMR spectra of **1a**−**3a** in $(CD_3)_2CO$ at 293 K show two sharp singlets (2:1) and two broad signals also with relative integrals 2:1 (see Figure 1a for the representative case of **1a**). The sharp singlets are due to the F_{ortho} (F^o) and F_{para} (F^p) nuclei of the starting material (complexes **a**). The broad signals were resolved at low temperature showing the presence of several complexes (see Figure 1b for **1a**), which are gathered in Table 1.

The colors of the solutions are pale yellow, and they do not show any variation with the temperature. In addition, the ^1H and ^{19}F NMR chemical shifts observed for the different species (similar to the ones found for Pd and Pt)[3] are those expected for diamagnetic compounds. We do not observe any indication for the presence of paramagnetic species (as should be expected for tetrahedral or octahedral complexes).

(8) (a) Carmona, E.; Marín, J. M.; Palma, P.; Paneque, M.; Poveda, M. L. *Inorg. Chem.* **1989**, *28*, 1895−1900. (b) Carmona, E.; Marin, J. M.; Paneque, M.; Poveda, M. L. *Organometallics* **1987**, *6*, 1757−1765. (c) Carmona, E.; Marin, J. M.; Palma, P.; Paneque, M.; Poveda, M. L. *Organometallics* **1985**, *4*, 2053−2055. (d) López, G.; García, G.; Sánchez, G.; García, J.; Ruiz, J.; Hermoso, J. A.; Vegas, A.; Martinez-Ripoll, M. *Inorg. Chem.* **1992**, *31*, 1518−1523.
(9) Jeener, J.; Meier, B. H.; Bachmann, P.; Ernst, R. R. *J. Chem. Phys.* **1979**, *71*, 4546−4553.
(10) Perrin, C. L.; Gipe, R. K. *J. Am. Chem. Soc.* **1984**, *106*, 4036−4038.
(11) Perrin, C. L.; Dwyer, T. J. *Chem. Rev.* **1990**, *90*, 935−967.
(12) See, for instance, (a) Geldbach, T. J.; Rüegger, H.; Pregosin, P. S. *Magn. Reson. Chem.* **2003**, *41*, 703−708. (b) Evans, D. R.; Huang, M.; Seganish, W. M.; Chege, E. W.; Lam, Y.-F.; Fettinger, J. C.; Williams, T. L. *Inorg. Chem.* **2002**, *41*, 2633−2641. (c) Frick, A.; Schulz, V.; Huttner, G. *Eur. J. Inorg. Chem.* **2002**, 3129−3147. (d) Catellani, M.; Meali, C.; Motti, E.; Paoli, P.; Perez-Carreño, E.; Pregosin, P. S. *J. Am. Chem. Soc.* **2002**, *124*, 4336−4346. (e) Cronin, L.; Higgitt, C. L.; Perutz, R. N. *Organometallics* **2000**, *19*, 672−683. (f) Alonso, M. A.; Casares, J. A.; Espinet, P.; Soulantica, K. *Angew. Chem., Int. Ed.* **1999**, *38*, 533−535. (g) Valentini, M.; Selvakumar, K.; Wörle, M.; Pregosin, P. S. *J. Organomet. Chem.* **1999**, *587*, 244−251. (h) Higgitt, C. L.; Klahn, A. H.; Moore, M. H.; Oelckers, B.; Partridge, M. G.; Perutz, R. N. *J. Chem. Soc., Dalton Trans*. **1997**, 1269−1280. (i) Wik, B. J.; Lersch, M.; Krivokapic, A.; Tilset, M. *J. Am. Chem. Soc.* **2006**, *128*, 2682−2696.
(13) Rausch, M. D.; Chang, Y. F.; Gordon, H. B. *Inorg. Chem.* **1969**, *8*, 1355−1362.
(14) Churchill, M. R.; Veidis, M. V. *J. Chem. Soc., Dalton Trans.* **1972**, 670−674.
(15) McDonald, R.; Sturge, K. C.; Hunter, A. D.; Shilliday, L. *Organometallics* **1992**, *11*, 893−900.
(16) Forniés, J.; Martín, A.; Menjón, B.; Kalamarides, H. A.; Rhodes, L. F.; Day, C. S.; Day, V. W. *Chem.−Eur. J.* **2002**, *8* (21), 4925−4934.

Table 1. ^{19}F NMR Chemical Shifts (ppm) for the Observed Species in $(CD_3)_2CO$ at 217 K

complex	δF^o (T_1, s)	δF^p
trans-[$NiRf_2(SbPh_3)_2$] (**1a**)	−86.57	−119.05
trans-[$NiRf_2(AsPh_3)_2$] (**2a**)	−88.21 (0.45)	−120.10
cis-[$NiRf_2(AsPh_3)_2$] (**2b**)	−90.25 (0.71)	−120.90
cis-[$NiRf_2(AsPh_3)\{OC(CD_3)_2\}$] (**2c**)	−89.66 (0.78), −91.51 (0.66)	−120.02, −121.34
trans-[$NiRf_2(AsCyPh_2)_2$] (**3a**)	−88.14	−119.96
cis-[$NiRf_2(AsCyPh_2)_2$] (**3b**)	−88.35	−119.43
cis-[$NiRf_2(AsCyPh_2)\{OC(CD_3)_2\}$] (**3c**)	−88.68, −91.58	−120.22, −121.12
trans-[$NiRf_2(AsMePh_2)_2$] (**4a**)	−88.92	−119.90
cis-[$NiRf_2(AsMePh_2)_2$] (**4b**)	−89.81	−121.42
trans-[$NiRf_2(PPh_3)_2$] (**5a**)	−87.60	−120.99
cis-[$NiRf_2\{OC(CD_3)_2\}_2$] (**6**)	−90.97 (0.71)	−120.30
cis-[$NiRf_2\{OC(CD_3)_2\}(OH_2)$] (**7**)	−89.84 (0.75), −90.03 (0.75)	−120.49, −120.69
cis-[$NiRf_2(OH_2)_2$] (**8**)	−89.20 (0.78)	−120.96

We could assign some of the signals to *cis*-[$NiRf_2\{OC(CD_3)_2\}_2$] (**6**), *cis*-[$NiRf_2\{OC(CD_3)_2\}(OH_2)$] (**7**), and *cis*-[$MRf_2(OH_2)_2$] (**8**), taking into account that their signals appeared for the three starting complexes **1a**−**3a** and their intensities were sensitive to the amount of water in solution.[17] The presence of uncoordinated ligand L was detected in each case by $^{13}C\{^1H\}$ NMR which confirmed a high degree of dissociation in all cases (98% for **1a**, 71% for **2a**, 48% for **3a**).

The assignment of the complexes detected in solution was made as follows: The resonances of coordinated H_2O were found in the ^1H NMR spectra at 5.32 and 5.34 ppm for **7** and **8**, respectively. The stereochemical assignment of a cis geometry for **7** was straightforward considering the inequivalence of the fluoroaryl rings and the strong coupling between the F^o of the two aryls.[18,19] Assignment of the cis geometry to **6** and **8** was also based on the exchanges observed between **6**, **7**, and **8** by ^{19}F EXSY experiments (see below) and the preference of the $NiRf_2$ moiety to form cis complexes with hard ligands.[16]

The trans isomer of [$NiRf_2(AsMePh_2)_2$] (**4a**) is in equilibrium with a small amount of the cis isomer (**4b**) in $(CD_3)_2CO$ at 217 K. In the ^{19}F NMR spectrum, the two fluoroaryl rings of **4b** are equivalent, and the ratio **4a**/**4b** did not change when small amounts of $AsMePh_2$ or H_2O were added to the solution. This discarded other formulations for **4b** such as [$NiRf_2(AsMePh_2)L$] (L = $(CD_3)_2CO$, H_2O).

No exchange, isomerization, or substitution processes were detected for *trans*-[$NiRf_2(PPh_3)_2$] (**5a**) in $(CD_3)_2CO$.

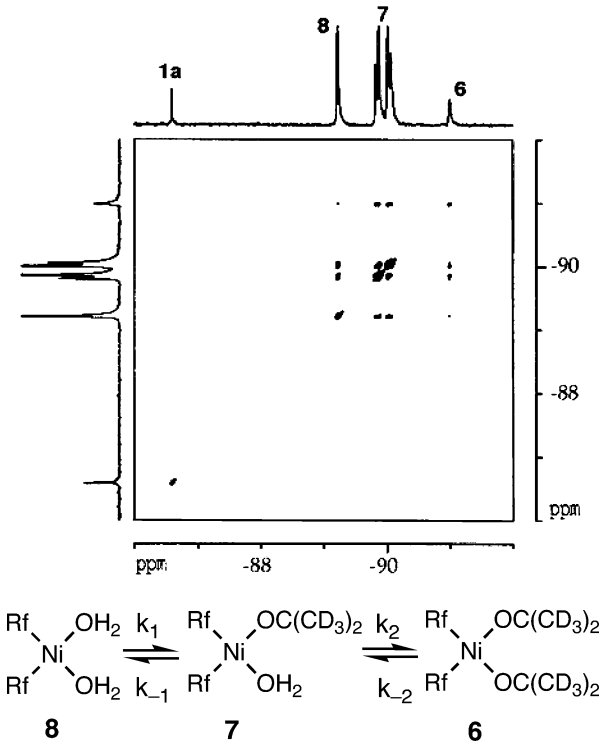

Figure 2. ^{19}F EXSY experiment in the F^o region for complex **1a** in wet $(CD_3)_2CO$ at 217 K (t_m = 0.2 s) and scheme of the exchange processes for **6**/**7**/**8**.

^{19}F EXSY Experiments for 1a−3a. When *trans*-[$NiRf_2(SbPh_3)_2$] (**1a**) is dissolved in $(CD_3)_2CO$, almost all of the complex is transformed into **6**, **7**, **8**, and uncoordinated $SbPh_3$. Only 2% remains as **1a**. The ^{19}F EXSY experiment at 217 K shows that **1a** does not participate in the exchange of **6**−**8** at this temperature (Figure 2). Therefore, we can analyze the latter, neglecting the presence of **1a**. In order to carry out this study, several phase-sensitive ^{19}F EXSY experiments were recorded in the F^o region at 217 K, with different mixing times (t_m = 0−0.3 s). The contour map of the spectrum obtained with a mixing time of 0.2 s is shown in Figure 2. The four resonances appearing along the diagonal at −89.2 (singlet), −89.8 and −90.0 (AB spin system), and −90.9 (singlet) correspond to **8**, **7**, and **6**, respectively. The stronger cross-peaks correlate with the single-step conversion of **8**/**7** and **7**/**6**. Lower intensity cross-peaks are due to the exchange between **8** and **6**. Since a simultaneous double substitution reaction is extremely unlikely, the latter exchange must proceed through **7** in a two-step process. In concordance with this, these cross-peaks do not appear in the spectra registered with very short mixing times, which is a commonly observed EXSY effect in multistep reactions.[20]

When *trans*-[$NiRf_2(AsPh_3)_2$] (**2a**) is dissolved in $(CD_3)_2CO$, the ^{19}F NMR spectrum at 217 K shows three F^o and three F^p signals in addition to those due to **2a** and **6**−**8**. These three new signals for each kind of F (ortho or para) are due to two new products **2b** (one signal) and **2c** (two signals with the same intensity). Altogether, 71% of $AsPh_3$ is dissociated. The addition of H_2O shifts the equilibria

(17) The formation of **7** and **8** is a consequence of the presence of small amounts of water in the commercial $(CD_3)_2CO$ used to prepare the NMR samples, which implies the presence of DHO and D_2O in equilibrium. Since Ni complexes with coordinated H_2O, DHO, or D_2O are not differentiated in the ^{19}F NMR, we consider them in practice as one compound. The same applies to $(CD_3)(CHD_2)CO$ molecules in the solvent. See also Experimental Section.

(18) Inter-aryl (including fairly large through-space) F−F couplings between F^o nuclei belonging to different fluoroaryl groups in the PdR_2 fragments have been reported: (a) Albéniz, A. C.; Casado, A. L.; Espinet, P. *Organometallics* **1997**, *16*, 5416−5423. (b) Alonso, M. A.; Casares, J. A.; Espinet, P.; Martínez-Ilarduya, J. M.; Pérez-Briso, C. *Eur. J. Inorg. Chem.* **1998**, 1745−1753. (c) De la Cruz, R.; Espinet, P.; Gallego, A. M.; Martín-Alvarez, J. M.; Martínez-Ilarduya, J. M. *J. Organomet. Chem.* **2002**, *663*, 108−177.

(19) Casares, J. A.; Espinet, P. *Inorg. Chem.* **1997**, *36*, 5428−5431.

(20) Heise, J. D.; Raftery, D.; Breedlove, B. K.; Washington, J.; Kubiak, C. P. *Organometallics* **1998**, *17*, 4461−4468.

completely to the formation of **7** and **8** while the addition of $AsPh_3$ shifts the equilibria toward **2a** and **2b**. Taking this into account, we assigned the above-mentioned signals to the following products: *cis*-[$NiRf_2(AsPh_3)_2$] (**2b**) with two equivalent fluoroaryl groups and *cis*-[$NiRf_2(AsPh_3)$-{$OC(CD_3)_2$}] (**2c**) with two inequivalent fluoroaryl groups and strong coupling between the F^o of the two aryls.

As observed for **1a**, the exchange between **2a** and any other complex is slow in the NMR time scale, but substitutions on its isomer **2b** take place easily (Figure 3). Apparently, the high trans effect of the haloaryl groups provides an efficient pathway for ligand substitution, and $AsPh_3$ is partially displaced by water or acetone.

Further support for the assignment of equilibria among **2b**, **2c**, and **6**−**8** came from the ^{19}F EXSY spectra. With a short t_m (0.15 s, Figure 3a), chemical exchange cross-peaks correlating **2c** signals with **2b** and **6** (corresponding to acetone−$AsPh_3$ and $AsPh_3$−acetone substitution processes, respectively) were observed. The cross-peaks due to $AsPh_3$−water exchange (**2c**−**7**) were not observable, indicating a very slow reaction. Using a longer t_m (0.45 s, Figure 3b), we obtained additional cross-peaks which correlate signals that exchange at a slower rate. Note that the new signals include the exchange of complexes involving the substitution of two ligands and also the exchange of the two nonequivalent fluoroaryl groups in complex **2c**.

The species observed when *trans*-[$NiRf_2(AsCyPh_2)_2$] (**3a**) is dissolved in $(CD_3)_2CO$ are similar to those observed for *trans*-[$NiRf_2(AsPh_3)_2$] (**2a**). Altogether, less dissociated $AsCyPh_2$ is produced (48%) than $AsPh_3$ (71%) for the case of **2a**, although the first substitution of L by $(CD_3)_2CO$ in the cis isomer is more favored for **3b** than for **2b** (see K_3 values in Table 2). The arsine substitution reactions (**3b**−**3c** and **3c**−**6** or **7**) are slower, and consequently no cross-peaks correlating these complexes were observed in the EXSY spectrum at 217 K, even at very large mixing times (Figure 4).

Considering the equilibria depicted in Figure 3 and the molar concentration of the different species detected in acetone solutions of **1a**, **2a**, and **3a**, we can calculate the equilibrium constants K_1−K_5 at 217 K (Table 2).

Rate Constant Calculations. The rate constants at 217 K for the dynamic exchange processes observed in solutions of **1a** and **2a** in commercial $(CD_3)_2CO$ and in $(CD_3)_2CO$/H_2O mixtures have been obtained (see Experimental Section) and are gathered in Table 2. The values obtained for **1a** in solutions with different amounts of water showed that the exchange rate $k_{7,8}$ is first order in free water ($k_{7,8} = k_{-1}$ [free water]). We assume that the dependence of $k_{6,7}$ on free water is the same, although this point cannot be experimentally supported because the signals due to **6** were not observable after the addition of small amounts of water. The larger k_1, k_{-1}, k_2, and k_{-2} values reported for **2a** compared to those reported for **1a** could arise in part from small differences in temperature and mostly from the limits of precision in the determination of the water concentration in commercial $(CD_3)_2CO$.

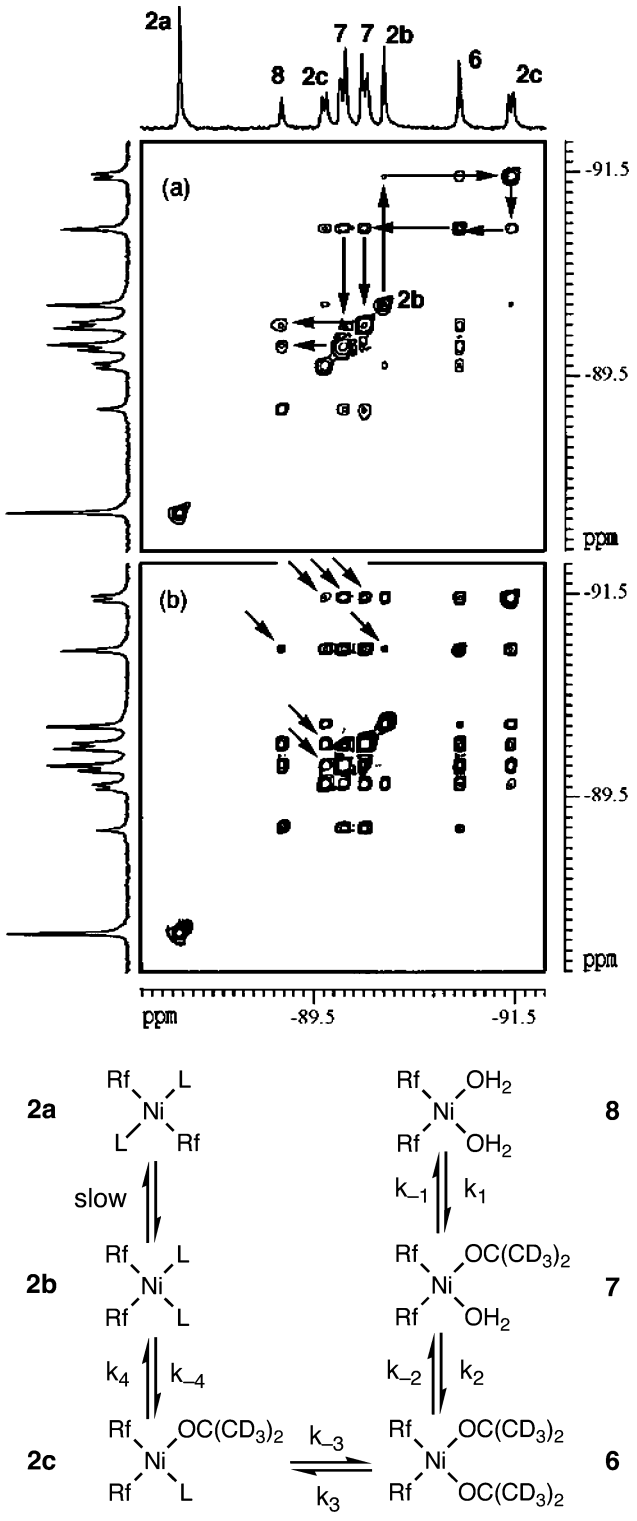

Figure 3. ^{19}F EXSY experiments in the F^o region of a solution of complex **2a** in wet $(CD_3)_2CO$ at 217 K ((a) $t_m = 0.15$ s, (b) $t_m = 0.45$ s) and scheme of the exchange processes between the different species formed. Arrows in (b) indicate the cross-peaks due to indirect exchanges (**2b**−**6**, **2c**−**7**, **6**−**8**, and the intramolecular exchange of the two nonequivalent fluoroaryls groups in **2c**).

The rate constant for the substitution of acetone by water in **7** to give **8** (k_{-1}) is two orders of magnitude higher than that for the substitution of water by acetone in **7** to give **6** (k_2/[acetone] = 0.074 M^{-1} s^{-1}). This reflects the higher lability of the coordinated acetone as compared to water. A

Table 2. Thermodynamic and Kinetic Data at 217 K for the Dynamic Exchange Processes Observed when **1a**−**3a** Were Dissolved in $(CD_3)_2CO$ (Errors in Parentheses)

equilibrium constants[a]			rate constants[b]		
	calculated from concentration data	calculated from the rate constants for **2a**		**1a**[c]	**2a**[d]
K_1	0.45 (0.12)	0.30 (0.04)	k_1	3.7 (0.8)	5.3 (0.4)
			k_{-1}	7.9 (0.6)	17.9 (0.9)
K_2	0.0106 (0.0007)	0.0081 (0.0006)	k_2	0.9	1.08 (0.06)
			k_{-2}	70.6	133 (3)
K_3	99 (4) (**2a**)	140 (50)	k_3		149 (4)
	382 (15) (**3a**)		k_{-3}		1.1 (0.4)
K_4	26.4 (1.1) (**2a**)	40 (11)	k_4		31 (3)
	8.0 (0.4) (**3a**)		k_{-4}		0.77 (0.14)
K_5	2.00 (0.04) (**2a**)				
	19.0 (0.4) (**3a**)				

[a] Equilibrium constants with units in parentheses: K_1 (M) = [**7**][H_2O]/[**8**] = k_1/k_{-1}, K_2 (M) = [**6**][H_2O]/[**7**] = k_2/k_{-2}, K_3 (M^{-1}) = [c]/[**6**][L] = k_3/k_{-3}, K_4 (M^{-1}) = [b]/[c][L] = k_4/k_{-4}, K_5 = [a]/[b]. [b] Constants k_1, k_2, k_{-3}, and k_{-4} in s^{-1}; k_{-1}, k_{-2}, k_3, and k_4 in M^{-1} s^{-1}. [c] Obtained from EXSY experiments (t_m = 0.15 s, [**1a**]$_0$ = 5.15 mM) carried out with different free water concentrations (47.1, 431.6, and 819.1 mM). [d] Obtained from eight EXSY experiments (t_m = 0.04−0.21 s); [**2a**]$_0$ = 11.02 mM, [free water] = 43.56 mM; [$AsPh_3$] = 13.66 mM. Free water concentration was calculated summing up [H_2O] + [DHO] + [D_2O] and subtracting the overall coordinated water for each sample.

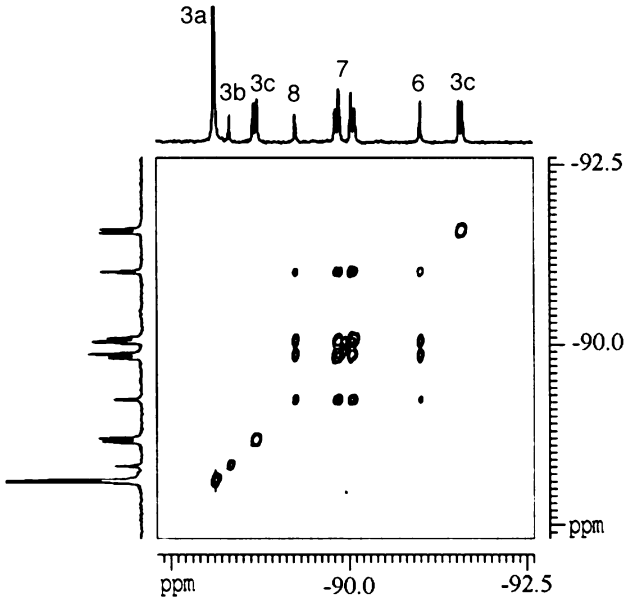

Figure 4. ^{19}F EXSY experiment in the F^o region for complex **3a** in wet $(CD_3)_2CO$ at 217 K (t_m = 0.5 s). The cross-peaks only correlate signals of **6**, **7**, and **8**.

similar result is observed when we compare the substitution of acetone by $AsPh_3$ and vice versa.

A deeper insight into the mechanism of these substitution reactions was obtained for the reaction **7** + $(CD_3)_2CO$ → **6** + H_2O. Its activation parameters were obtained using line shape analysis for **1a** to determine the values of k_2 at different temperatures. The values obtained were $\Delta H^{\ddagger}$ = 39.1 ± 0.7 kJ mol^{-1} and $\Delta S^{\ddagger}$ = −64 ± 3 J mol^{-1} K^{-1}. The negative value of $\Delta S^{\ddagger}$ is indicative of an associative substitution.[21]

The complexes reported here afford the only study available to date on square-planar Ni(II) aquacomplexes. However, the substitution rates observed should be used with some caution when comparing to other systems, as the high trans effect of the Rf groups is probably reducing the activation energy toward associative ligand substitution, compared to the classical inorganic ligands used in Ni(II) octahedral complexes (these Rf ligands were, however, needed to induce a square-planar coordination in Ni(II)). In this respect, it is interesting to note that the fast ligand substitutions take place on the cis isomers (where the leaving ligand is trans to Rf) and not on the initial trans isomers.

The use of a better donor and less labile ligand than $AsPh_3$ ($AsCyPh_2$) slows the substitution processes down to the point that they cannot be detected experimentally in the same conditions. For similar electronic characteristics, displacement of a less bulky ligand ($AsMePh_2$) is clearly disfavored.

All of these data fit well with the behavior observed for these complexes as catalysts in the insertion polymerization of norbornene. A prerequisite for insertion polymerization is efficient ligand substitution by an incoming norbornene, which then coordinates by its double bond and undergoes insertion.[4] The yield and molecular mass of the polymers obtained with these catalysts show a strong dependence on the ligand used and the solvent. High yield and high molecular mass values were obtained with the ligands shown here which were easier to displace. Furthermore, solvents with hard donor atoms which, as shown here, give more stable complexes were detrimental for polymerization.

Experimental Section

General Methods. All reactions were carried out under N_2. Solvents were distilled using standard methods. The nickel compounds were prepared by published methods.[4] ^1H (300.13 MHz), ^{19}F (282.40 MHz), and $^{13}C\{^1H\}$ (75.47 MHz) NMR spectra were recorded on Bruker ARX 300 and AC 300 instruments equipped with a VT-100 variable-temperature unit. The actual temperature was measured before spectral accumulation, using Bruker standard samples of methanol in methanol-d_4 for low temperatures and ethylene glycol in DMDO-d_6 (80/20) for high temperatures and using the equations provided by the manufacturer. Chemical shifts are reported in parts per million from $SiMe_4$ (^1H, $^{13}C\{^1H\}$) or CCl_3F (^{19}F) with positive shifts downfield, at an ambient probe temperature unless otherwise stated. J values are given in hertz. ^{19}F EXSY experiments were carried out with a standard nuclear Overhauser effect spectroscopy (NOESY) program operating in phase sensitive mode, with a 5% random variation of the evolution time to avoid correlation spectroscopy (COSY) cross-peaks. T_1 values were obtained using a standard inversion recovery sequence.

$(CD_3)_2CO$ was used as received, and the total water content in it ([H_2O] + [HDO] + [D_2O]) was calculated from the integrated area values of H_2O (2.84 ppm) and HDO (2.80 ppm, $^2J_{H-D}$ = 1.1 Hz) in the ^1H NMR spectra of a commercial sample and using the equilibrium constant K_{eq} = 3.81 for the self-exchange reaction H_2O + D_2O = 2HDO.[22]

(21) Monlien, F. J.; Helm, L.; Abou-Hamdan, A.; Merbach, A. E. *Inorg. Chem.* **2002**, *41*, 1717−1727 and references therein.

(22) Chen, C. L.; Bopp, P.; Wolfsberg, M. *J. Chem. Phys.* **1982**, *77*, 579−580.

The mathematical analysis to extract rate constants from 2D-EXSY experiments has been carefully summarized in the review by Perrin and Dwyer.[11] For a multispin system undergoing chemical exchange, the peak intensities are given by eq 1, where **I** is the matrix of cross-peak intensities I_{ij}, **M**° is the matrix of equilibrium magnetizations of the nulei, **R** is the relaxation matrix, and t_m is the mixing time used for acquisition of the spectrum.

$$\mathbf{I} = \mathbf{M}^\circ \exp(-\mathbf{R}t_m) \quad (1)$$

The matrix **I** for each spectrum was obtained with the values of peak volumes I_{ij}. The experimental values at both sides of the diagonal (I_{ij}(exp) and I_{ji}(exp)), which were integrated with the standard Bruker software, were not symmetrized. The matrix **M**° was constructed with the integrated values of the diagonal peak volumes at $t_m = 5$ μs.

For complex **7**, we have considered jointly the AB system because this simplifies the spin problem (from a four site to a three site exchange system for the exchange **6**/**7**/**8**) and also eliminates the errors introduced from *J* cross-peaks (which has to be taken into account particularly if $\Delta\nu < 20J$) and from cross-relaxation.[11,12e]

The computer simulation of the variable temperature NMR spectrum of a solution of **1a** in $(CD_3)_2CO$ was carried out by line shape analysis using the standard program gNMR.[23]

Acknowledgment. Financial support by the Ministerio de Ciencia y Tecnología (Project No. CTQ2004-07667), the Junta de Castilla y León (Project No. VA060/04), and Consolider Ingenio 2010 (Grant CSD2006-0003) is very gratefully acknowledged.

Supporting Information Available: Percentages of the different species which arise from the solution of *trans*-[$NiRf_2L_2$] in $(CD_3)_2CO$ at 217 K in different conditions, thermodynamic and kinetic data (exchange rates and rate constants) at 217 K for the dynamic exchange processes observed when **1a**−**3a** were dissolved in $(CD_3)_2CO$, rate constants (k_2) for the reaction **7** + $(CD_3)_2CO$ → **6** + H_2O obtained by line shape analysis, analysis section, microprogram (Matlab) for rate calculations. This material is available free of charge via the Internet at http://pubs.acs.org.

IC061933K

(23) *gNMR*, version 3.6 for Macintosh; IvorySoft, Cherwell Scientific Publishing, Ltd.: Oxford, U.K., 1995.